# Role of plasma membrane-bound sialidase NEU3 in clathrin-mediated endocytosis

**Macarena Rodriguez-Walker*[1], Aldo A. Vilcaes*[1], Eduardo Garbarino-Pico* and José L. Daniotti*[2]**

*Centro de Investigaciones en Química Biológica de Córdoba (CIQUIBIC, UNC-CONICET), Departamento de Química Biológica, Facultad de Ciencias Químicas, Universidad Nacional de Córdoba, Córdoba, Argentina.

[1] These authors contributed equally to this article.

[2] Corresponding author: José Luis Daniotti, Facultad de Ciencias Químicas, Haya de la Torre y Medina Allende, Ciudad Universitaria, UNC, X5000HUA, Córdoba, Argentina. Tel.: 54-351-5353850 ext. 3447; Fax: 54-351-4334074; e-mail: daniotti@dqb.fcq.unc.edu.ar

**Short title**: Sialidase NEU3 modulates clathrin-mediated endocytosis

**Abbreviations**: CHO, Chinese hamster ovary; CME, Clathrin-mediated endocytosis; Tf, transferrin; CTx, cholera toxin; CTxβ, cholera toxin β-subunit; LDL, low-density lipoprotein; $\alpha_2$M, $\alpha_2$ Macroglobulin; ST8Sia-I, CMP-NeuAc:GM3 sialyltransferase; β4GalNAcT-I, UDP-GalNAc:LacCer/GM3/GD3/GT3 β-1,4-*N*-acetylgalactosaminyltransferase; β3GalT-IV, UDP-Gal:GA2/GM2/GD2 β-1,3galactosyl transferase; P4, D,L-threo-1-fenyl-2-hexadecanoilamino-3-pirrolidino-1-propanol-HCl; CLC, clathrin light chain; PtdIns(4,5)$P_2$, phosphatidylinositol (4, 5)-bisphosphate; AP-2, clathrin adaptor protein 2; Cer, Ceramide; GM3, NeuAcα2,3Galβ1,4Glc-Cer; GD3, NeuAcα2,8NeuAcα2,3Galβ1,4Glc-Cer; GT3, NeuAcα2,8NeuAcα2,8NeuAcα2,3Galβ1,4Glc-Cer; GM1, Galβ1,3GalNAcβ1,4(NeuAcα2,3) Galβ1,4Glc-Cer; GD1a, NeuAcα2,3Galβ1,3GalNAcβ1,4(NeuAcα2,3) Galβ1,4Glc-Cer.

## ABSTRACT

Gangliosides are sialic acid containing glycosphingolipids mainly expressed at the outer leaflet of the plasma membrane. Sialidase NEU3 is a key enzyme in the catabolism of gangliosides with its up-regulation having been observed in human cancer cells. In the case of clathrin-mediated endocytosis (CME), although this has been widely studied, the role of NEU3 and gangliosides in this cellular process has not yet been established. Here, we found an increased internalization of transferrin (Tf), the archetypical cargo for CME, in cells expressing complex gangliosides with high levels of sialylation. The ectopic expression of NEU3 led to a drastic decrease in Tf endocytosis, suggesting a participation of gangliosides in this process. However, the reduction of Tf endocytosis caused by NEU3 was still observed in glycosphingolipid-depleted cells, indicating that NEU3 could operate in a way that is independent of its action on gangliosides. Additionally, internalization of $\alpha_2$ macroglobulin and low-density lipoprotein, other typical ligands in CME, was also decreased in NEU3 expressing cells. In contrast, cholera toxin β-subunit internalization, which is endocytosed by both clathrin-dependent and clathrin-independent mechanisms, remained unaltered. Kinetic assays revealed that NEU3 caused a reduction in the sorting of endocytosed Tf to early and recycling endosomes, with the Tf binding at the cell surface being also reduced. NEU3 expressing cells showed an altered subcellular distribution of clathrin adaptor AP-2, but did not reveal any changes in the membrane distribution of clathrin, phosphatidylinositol (4, 5)-bisphosphate or caveolin-1. Overall, these results suggest a specific and novel role of NEU3 in CME.

**Summary statement**: Sialidase NEU3 is a key enzyme in the catabolism of gangliosides. We demonstrated that NEU3 impairs cargoes internalization via clathrin-coated pits, affecting AP-2 subcellular distribution. This study delineates previously unidentified cellular functions of NEU3.

**Key words:** glycolipid; sialidase; ganglioside; clathrin; membrane trafficking; NEU3

## INTRODUCTION

Endocytosis is an essential process for diverse cellular functions such as nutrient uptake, cell communication, plasma membrane remodeling and internalization of lipids and receptor bound macromolecules [1, 2]. Several entry pathways into cells have been identified, which vary in the cargoes they transport and in the protein and lipid machinery that facilitate the endocytic process.

Clathrin-mediated endocytosis (CME) constitutes the principal and best characterized route for selective receptor internalization in higher eukaryotic cells [3]. More recently, however, several endocytic pathways that do not use clathrin have also been reported. These pathways, constitutive or triggered by specific signals, often differ in their mechanism of formation, molecular machinery and cargo destination [4-7].

Gangliosides, which are sialylated glycosphingolipids, are key signaling molecules in biological events that have been implicated in many physiological processes, including growth, signaling, migration, membrane trafficking and apoptosis. Moreover, some ganglioside functions are undesirable, as they are receptors for viruses, toxins, and antibodies [8-10]. Gangliosides are typically anchored in the outer leaflet of the plasma membrane and are widely found in vertebrate tissues. Their de novo synthesis starts at the endoplasmic reticulum and is continued by a combination of glycosyltransferase activities at the Golgi complex, followed by vesicular delivery to the plasma membrane [11, 12]. At the cell surface, gangliosides can undergo endocytosis, and once internalized, they can be sorted into endosomes or degraded by glycohydrolases at the lysosomal level. Recently, a number of enzymes for ganglioside anabolism and catabolism have been shown to be associated with the plasma membrane, which were able to exert their enzymatic activities on substrates belonging to the surface of both their own and neighboring cells [13-16]. It has been hypothesized, and in some cases clearly demonstrated, that these activities are responsible for the fine tuning of the plasma membrane ganglioside composition, and consequently, the functional properties of plasma membrane proteins involved in different signaling processes [17, 18].

Sialidases are glycohydrolases that catalyze the removal of α-glycosidically linked sialic acid residues from carbohydrate groups of glycoproteins and glycolipids. Four types of mammalian sialidases have been identified and characterized to date, which have been designated as NEU1, NEU2, NEU3 and NEU4. They are encoded by different genes and differ in major subcellular localization and enzymatic properties. In particular, NEU3 is mainly expressed at the plasma membrane and is a key enzyme in the catabolism of membrane gangliosides. For this reason, NEU3 has been implicated in similar processes to those involving gangliosides, such as adhesion, differentiation, cancer progression and apoptosis [17, 19-21]. A remarkable up-regulation (3 to 100-fold) of NEU3 has been observed in various human cancer cells, in which a high concentration of the enzyme regulates transmembrane signaling at the plasma membrane, through both the modulation of ganglioside expression and by direct interaction with signal molecules such as epidermal growth factor receptor [22, 23]. In addition, NEU3 has been described to be closely associated with caveolin-1 in membrane microdomains [24] with its silencing enhancing the caveolar endocytosis of β1 integrin, blocking its recycling and reducing its levels at the cell surface [25]. On the other hand, while we were examining endocytosis in a panel of cell lines genetically modified to express different ganglioside species, we observed that expression of complex and highly sialylated gangliosides correlates with an increased internalization of cargoes via CME. Thus, to further investigate the participation of gangliosides in endocytic processes, we decided to study the consequences of their desialylation, by expression of the sialidase NEU3. Our results show that: (*a*) the ectopic expression of human NEU3 led to a drastic decrease in the CME of transferrin (Tf), low-density lipoprotein (LDL) and $\alpha_2$

Macroglobulin ($\alpha_2$M); (*b*) the up-expression of NEU3 did not modify the clathrin-independent endocytosis of cholera toxin (CTx); (*c*) most of the NEU3 effect on the Tf internalization is independent of its catabolic activity towards gangliosides; *(d)* the effect produced by NEU3 on CME involved an abnormal distribution of the clathrin adaptor AP-2, whereas the intracellular distribution of clathrin, PtdIns(4,5)$P_2$ and caveolin-1 remained unchanged. Overall, these results suggest a specific and novel role of NEU3 in CME and indicate that the sialidase might play crucial roles in regulation of cell surface functions besides ganglioside catabolism.

## EXPERIMENTAL

### Expression plasmids

The constructs containing the DNA coding sequence for human NEU3 tagged at the C-terminus with the epitope c-Myc (NEU3) were obtained by subcloning the corresponding DNA fragments into the pCI-neo (Promega, Madison, WI, USA) or pTracer-CMV (Invitrogen, CA, USA) mammalian expression vectors. Expression plasmids for wild type GTPase Rab11a-GFP, wild type GTPase Rab5-GFP, lysosome-associated membrane protein 1 (LAMP1)-GFP and glycosyltransferase β4GalNAcT-I-Cherry have been already described elsewhere [26-28]. Plasmids coding for clathrin adaptor AP-2 σ2 subunit (AP-2)-GFP and clathrin light chain (CLC)-EYFP were generously supplied by J. Bonifacino (NICHD, National Institutes of Health, Bethesda, MD, USA) [29]. Plasmid PH-PLCδ1-RFP encoding pleckstrin homology domain of phospholipase Cδ1 fused to red fluorescent protein was kindly supplied by S. Grinstein (Department of Cell Biology, The Hospital for Sick Children, Toronto, ON, Canada).

### Cell lines and cell cultures

The following cells were used: Wild-type CHO-K1 cells (CHO-K1$^{GM3+}$) (ATCC, Manassas, VA, USA); CHO-K1 clone 2 (CHO-K1$^{GD3+}$), a stable chick CMP-NeuAc: GM3 sialyltransferase (ST8Sia-I, also called Sial-T2) transfectant expressing the gangliosides GD3 and GT3 [30]; CHO-K1 clone 4 (CHO-K1$^{GD1a+}$), a stable double transfectant expressing UDP-GalNAc:LacCer/GM3/GD3/GT3 β-1,4-*N*-acetylgalactosaminyltransferase (β4GalNAcT-I, also called GalNAc-T) and UDP-Gal:GA2/GM2/GD2 β-1,3galactosyl transferase (β3GalT-IV, also called Gal-T2) [30] and having an increased expression of GM1 and GD1a; and COS-7 cells. Cells were grown and maintained at 37°C in 5% $CO_2$ in DMEM (Dulbecco's Modified Eagle Medium; Invitrogen, CA, USA) supplemented with 10% FBS and antibiotics. Transfections were carried out with 1 µg per 35-mm dish of the indicated plasmid using cationic liposomes (Lipofectamine; Invitrogen, CA, USA) or polyethylenimine (PEI, Sigma-Aldrich, St. Louis, MO, USA). CHO-K1$^{GM3+}$, CHO-K1$^{GD3+}$ and CHO-K1$^{GD1a+}$ cells transiently transfected with pCI-neoNEU3 are referred to as CHO-K1$^{GM3+,\ NEU3+}$, CHO-K1$^{GD3+,\ NEU3+}$ and CHO-K1$^{GD1a+,\ NEU3+}$ cells, respectively. CHO-K1$^{GM3+}$ cells transiently transfected with pTracerNEU3 (which expresses NEU3 and GFP under independent promoters) are referred to as CHO-K1$^{GM3+,\ GFP(NEU3)+}$, with GFP expression being used as a marker to identify NEU3 expressing cells. Clones with stable expression of CLC-EYFP or AP-2-GFP were generated in CHO-K1$^{GM3+}$ cells.

To generate stably NEU3 expressing cells, CHO-K1$^{GM3+}$ cells were transfected with pTracerNEU3. Then, cells were sorted according to their GFP expression using a FACS CantoII cytometer (BD Biosciences, San Jose, CA, USA) and cells with higher expression of GFP were collected. Stably-transfected cells were selected by the addition of Zeocin (Invitrogen, CA, USA) as a selection marker. This mixed population of antibiotic resistant cells was checked for NEU3 expression and used directly for experimental analysis.

### Antibodies

The following antibodies were used: monoclonal mouse antibody to human NEU3 *(*MBL International Corporation, Woburn, MA, USA); monoclonal and polyclonal antibodies to c-Myc produced in mouse and rabbit, respectively (Sigma-Aldrich, St. Louis, MO, USA); polyclonal rabbit antibody to caveolin-1 (Abcam, Cambridge, MA, USA), monoclonal mouse antibody to GD3 (clone R24, ATCC, Manassas, VA, USA), monoclonal mouse antibody to GD1a (kindly supplied by P.H. Lopez, INIMEC-CONICET, Córdoba, Argentina), monoclonal mouse antibody to tubulin (Sigma-Aldrich, St. Louis, MO, USA) and monoclonal mouse antibody to GFP (Roche, Indianapolis, IN, USA). The secondary antibodies used were Alexa$^{488}$-conjugated goat anti-mouse IgG, Alexa$^{546}$-conjugated goat anti-mouse IgG, Alexa$^{568}$-conjugated goat anti-mouse IgG, Alexa$^{546}$-conjugated goat anti-rabbit IgG (Molecular Probes, Eugene, OR, USA) for immunofluorescence and goat anti-rabbit or mouse IgG coupled to IRDye800CW (LI-COR Biotechnology, Lincoln, NE, USA) for Western blotting.

### Immunofluorescence staining and confocal microscopy analysis

Immunofluorescence experiments were performed as described previously [27], with minor modifications. Cells were seeded onto glass coverslips and transfected with NEU3 and with Rab5-GFP, Rab11a-GFP, β4GalNAcT-I-Cherry, LAMP1-GFP, CLC-EYFP, AP-2-GFP or PH-PLCδ1-RFP when indicated. At 24 h post-transfection, cells were analyzed in vivo by confocal microscopy or fixed with 1% paraformaldehyde in PBS for 10 min. After washes with PBS, cells were incubated with primary and secondary antibodies. In some cases, cells were permeabilized with 0.1% Triton X-100/200 mM glycine in PBS for 2 min at room temperature. Nuclei were stained blue with Hoechst 33258 dye (Molecular Probes, Eugene, OR, USA). For staining of the plasma membrane associated gangliosides, cells were incubated with antibody to GD3, antibody to GD1a or CTx β-subunit (CTxβ, which binds to GM1) at 4°C for 60 min prior to fixation. Confocal images were collected using an Olympus FluoView FV1000 confocal microscope (Olympus Latin America, Miami, FL, USA) equipped with an argon/helium/neon laser and a 63x (numerical aperture = 1.4) oil immersion objective (Zeiss Plan-Apochromat). Single confocal sections of 0.8 μm were taken parallel to the coverslip (*xy* sections). In some cases, confocal slices of 0,2 μm were taken perpendicular to the image plane (z-slices).

### Image processing

Final images were compiled with Adobe Photoshop CS4, with the confocal fluorescence micrographs shown in this manuscript being representative of at least three independent experiments. Scale bars in all figures: 10 μm. Quantification of fluorescence intensity (arbitrary units/cell area) of a focal plane of at least 20 cells of each experimental condition was performed using ImageJ software. Quantification of the number of clathrin, AP-2 and caveolin-1 pits of at least 20 cells of each experimental condition was performed using Particle Analysis ImageJ plugin. Manders' co-localization coefficients were calculated using JACoP ImageJ plugin with at least 10 cells of each experimental condition being imaged on the *z* axis (5 to 10 z-slices).

### Cargo internalization assays

For internalization experiments using Alexa$^{647}$-conjugated human transferrin (Tf-Alexa$^{647}$, Molecular Probes, Eugene, OR, USA), cells grown on coverslips and transfected to express NEU3 were first incubated for 60 min at 37°C in DMEM without FBS in order to deplete serum Tf. Then, cells were incubated for 45 min at 37°C with pre-warmed DMEM, without FBS, supplemented with 4 μg/ml of Tf-Alexa$^{647}$. To concentrate the cargo at early endosomes [31], cells were incubated with DMEM containing 4 μg/ml Tf-Alexa$^{647}$ at 16°C for 30 min. To avoid endocytosis and to concentrate Tf mainly at the cell surface, cells were incubated

with DMEM containing 4 μg/ml Tf-Alexa$^{647}$ at 4°C for 30 min. 0.6% BSA was used in all experiments of Tf binding and uptake. After washes with cold PBS, cells were analyzed in vivo by confocal microscopy or fixed and immunostained as described above. For endocytosis experiments using Alexa$^{594}$-conjugated $\alpha_2$M ($\alpha_2$M-Alexa$^{594}$; generously supplied by G. Chiabrando, CIBICI-CONICET, National University of Córdoba, Argentina), fluorescent LDL (BODIPY-LDL; generously supplied by C. Touz, INIMEC-CONICET, Córdoba, Argentina) and Alexa$^{555}$-conjugated CTxβ (CTxβ-Alexa$^{555}$; Molecular Probes, Eugene, OR, USA), the NEU3 expressing cells were first incubated for 60 min at 37°C in DMEM without FBS and then with prewarmed DMEM supplemented with $\alpha_2$M-Alexa$^{594}$ (60 nM), BODIPY-LDL (8 μg/ml) or CTxβ (0.2 μg/ml) for 30 min at 37°C. Finally, cells were washed, fixed in 1% paraformaldehyde and processed for immunofluorescence and confocal microscopy.

### Ganglioside and phosphoinositide depletion

To reduce GM3, GD3 and the neutral glycosphingolipid content, cells were treated with 2.4 μM of d,l-threo-1-phenyl-2-hexadecanoylamino-3-pyrrolidino-1-propanol-HCl (P4) (Matreya Inc., PA, USA) [30]. After P4 treatment, cells were transfected to express NEU3 and then subjected to Tf internalization at 37°C as indicated above. Hydrolysis of phosphoinositides was initiated by the addition of 10 μM ionomycin (Sigma-Aldrich, St. Louis, MO, USA) in the presence of 1.5 mM external calcium for 1 minute at 37°C. PtdIns(4,5)$P_2$ hydrolysis is reflected in the redistribution of the probe fluorescence from the plasma membrane into the cytosol [32].

### Western blotting

Cell homogenates were resolved by electrophoresis through 12% SDS-polyacrylamide gels under reducing conditions. Proteins were electrophoretically transferred to nitrocellulose membranes. For immunoblotting, non-specific binding sites on the nitrocellulose membrane were blocked with 5% defatted dry milk in 400 mM NaCl, 100 mM Tris-HCl, pH 7.5. A mouse antibody to c-Myc or an antibody specific to NEU3 was used. Bands of proteins were detected using Odyssey infrared imaging system (LI-COR Biotechnology, Lincoln, NE) with goat antibody to rabbit or mouse IgG coupled to IRDye800CW (LI-COR Biotechnology, Lincoln, NE). Molecular mass were calculated based on calibrated standards (Spectra Multicolor Broad Range Protein Ladder; Life technologies) run in every gel. For subcellular fractionation, cells were mechanically lysed and the homogenates were ultra-centrifuged at 90000 rpm. NEU3 expression in both supernatant (S) and pellet (P) fractions was determined by Western blot using an antibody to NEU3. For internalization experiments using Tf-Alexa$^{647}$, cells stably expressing NEU3 were first incubated for 60 min at 37°C in DMEM without FBS in order to deplete serum Tf. Then, cells were incubated for 45 min at 37°C with pre-warmed DMEM, without FBS, supplemented with 0.75 μg/ml Tf-Alexa$^{647}$. After washes with cold PBS, cells were acid stripped with 0.5% acetic acid buffer, pH 3.5, containing 0.5 M NaCl for 5 min on ice and scrapped from the plate. Next, the homogenates were mechanically lysed and resolved by electrophoresis as described above. The Tf-Alexa$^{647}$ transferred to nitrocellulose membranes was directly detected taking advantage of its near-infrared fluorescence. Tubulin was used as a loading control. The images were obtained using Odyssey Application Software version 2.1., with the final ones being compiled with Adobe Photoshop CS4.

### Statistical analyses

Data are presented as the mean±SEM. Statistical analyses were made using Student's t-test or ANOVA with SigmaPlot 11.0 software. Significance (*) was attributed at the 95% level of confidence ($p<0.05$).

### RNA isolation and cDNA synthesis

Total RNA was purified using TRIzol reagent (Invitrogen, CA, USA) according to the manufacturer's instructions. Five microgram of total RNA was utilized as template for the cDNA synthesis reaction using SuperScript™ III Reverse Transcriptase (Invitrogen) and a blend of oligo(dT) and random hexamers (Biodynamics, Buenos Aires, Argentina) according to the manufacturer's instructions.

### Real-time quantitative PCR

SYBR Green based Real Time qPCR was achieved as reported before [33]. Primers specific to CHO-K1 endogenous *NEU1*, *NEU2* and *NEU3* were designed and purchase from Invitrogen (CA, USA). The quantifications were performed in Rotor-Gene Q equipment (Qiagen, Hilden, Germany). The amplification mix contained 1 µL of the cDNA synthesis reaction, 0.8 mM of each primer and 7.5 µL of Real Mix (Biodynamics, Buenos Aires, Argentina) in a total volume of 15 µL. The cycling conditions were 30 sec polymerase activation at 95°C and 40 cycles of 95°C for 30 sec, 60°C for 30 sec and 72°C for 30 sec. Each assay included a standard curve in duplicate, utilizing 1:5 serial dilutions of cDNA from CHO-K1$^{GM3+}$ cells. Samples were measured in triplicate. The PCR product was checked by melt curve analysis, and the standard curve linearity and PCR efficiency were optimized. The data was analyzed with Rotor-Gene Q software (Qiagen, Hilden, Germany). The relative concentration values were normalized by the geometric average of three internal control genes: *Tbp*, *GAPDH*, and *18S rRNA* [34].

### Metabolic labeling, lipid extraction and chromatography

Briefly, cells grown in 35-mm dish were labeled with 30 µCi/ml [$^3$H]galactose for 24 h. After washing with cold PBS, cells were scraped from the plate and pelleted by centrifugation. Lipids were extracted from the cell pellet with chloroform:methanol (2:1 v/v) and freed from water-soluble contaminants by passing through a Sephadex G-25 column. The lipid extracts and standards were chromatographed on high performance thin-layer chromatography (HPTLC) plates (Merck Millipore, Darmstadt, Germany) using chloroform:methanol: 0.25% $CaCl_2$ (60:36:8 v/v) as solvent. Standard gangliosides were visualized by exposing the plate to iodine vapors. Radioactive gangliosides (10,000 cpm on each lane) were visualized by fluorography after dipping the plate in 0.4% melted 2,5-diphenyloxazole in 2-methylnaphthalene and exposure to a radiographic film at -70 °C.

## RESULTS

### Expression of complex and highly sialylated gangliosides correlates with an increased internalization of Tf

First of all, we examined the endocytosis of Tf, the archetypical cargo for internalization through CME, in a panel of CHO-K1 cell lines genetically modified to express different ganglioside species [30] (Fig. 1A). Wild type CHO-K1 cells express predominantly the monosialo-ganglioside GM3 (CHO-K1$^{GM3+}$). Cells stably transfected with the cDNA encoding ST8Sia-I synthesizes mainly the disialo-ganglioside GD3 and to a lesser extent the trisialo-ganglioside GT3 but practically do not synthesize GM3 (CHO-K1$^{GD3+}$). On the other hand, CHO-K1 cells stably expressing the enzymes β4GalNAcT-I and β3GalT-IV mainly synthesize the a-serie ganglioside GD1a and to a lesser extent GM1 (CHO-K1$^{GD1a+}$) (Fig. 1B).

Tf internalization in these cells was investigated at 37°C for 45 min as indicated in the Experimental section. Confocal microscopy analysis revealed a variable Tf cellular endocytosis, which was positively correlated with the degree of ganglioside complexity and sialylation level (GM3<GD3<GD1a) (Fig. 1C). It is worth to mention that under the

experiential conditions used in this assay, Tf is internalized by cells and is mainly accumulated in recycling endosomes. Thus, these results suggest the participation of gangliosides in the endocytic process of Tf.

### Characterization of ectopically expressed human NEU3

To investigate the participation of gangliosides in the endocytosis of Tf, and taking into account the positive correlation between the degree of ganglioside sialylation and Tf endocytosis, we decided to study the consequences of ganglioside desialylation in the endocytic process by expression of the sialidase NEU3. First, we performed a detailed biochemical and cellular characterization of ectopically expressed human NEU3 tagged at the C-terminal with the c-Myc epitope. Extracts from NEU3 transiently transfected CHO-K1$^{GM3+}$ cells analyzed by Western blotting with anti-c-Myc antibodies showed NEU3 migrating with the expected molecular mass of 56 kDa. A similar result was observed using a monoclonal antibody specific to human NEU3 (Fig. 2A). No immunostained band was observed in extracts from non-transfected CHO-K1$^{GM3+}$ cells. More than 98% of the expressed sialidase was recovered in the rough particulate fraction obtained by ultracentrifugation (Fig. 2B). As previously reported [35], NEU3 was mainly localized at the plasma membrane (Fig. 2C). In addition, NEU3 was also found to localize in membranes from lysosomes (LAMP1$^{+}$), recycling endosomes (Rab11$^{+}$) and early endosomes (Rab5$^{+}$). However, NEU3 did not colocalize with β4GalNAcT-I, a Golgi marker (Fig. 2D). In all cases, the organelle markers revealed the typical morphology and intracellular distribution in CHO-K1$^{GM3+}$ cells expressing NEU3, allowing us to discard any changes at this level being associated with the expression of the sialidase. Next, we evaluated the NEU3 enzymatic activity. Since gangliosides GD3 and GD1a can be detected with specific monoclonal antibodies, we investigated the enzymatic activity of NEU3 on GD3 and GD1a substrates in CHO-K1$^{GD3+}$ and CHO-K1$^{GD1a+}$ cells, respectively. As shown in Figure 2E, NEU3 expression resulted in a clear and significant decrease in the GD3 and GD1a content, with a concomitant increase in the content of the product GM1 in CHO-K1$^{GD1a+}$ cells, whose inner sialic acid residue is not accessible for NEU3 activity. Additionally, in CHO-K1$^{GD3+}$ cells transiently expressing NEU3 sialidase, the ex vivo activity was found to be 60% higher than in mock transfected cells using 4-methylumbelliferyl-α-D-N-acetylneuraminic acid (4-MU-NeuAc) as the substrate at pH 4.5 (data not shown). Taken together, results from these experiments indicate that the expressed sialidase was enzymatically active.

### Plasma membrane-bound sialidase NEU3 impairs the CME of Tf

Having fully characterized NEU3 expression, we next investigated its role in modulating endocytosis of Tf. To carry this out, cells expressing different species of gangliosides were transiently transfected to express NEU3. Interestingly, we observed by confocal microscopy analysis that the Tf uptake drastically decreased in CHO-K1$^{GM3+}$, CHO-K1$^{GD3+}$ and CHO-K1$^{GD1a+}$ cells ectopically expressing NEU3 (Fig. 3A and B). Moreover, a similar effect on Tf endocytosis was also observed in COS-7 cells expressing human NEU3 (Supplemental Fig. S1). A similar result was also obtained in CHO-K1 cell lines stably expressing human NEU3, in which Tf endocytosis was quantified using volumetric fluorescence quantification in 3D-reconstituted imaging (not shown) and by a biochemical approach (Fig. 3C). Overall, these results suggest a participation of gangliosides in the endocytic process of Tf, which was drastically affected by expression of the sialidase NEU3.

To analyze further the participation of gangliosides in the CME of Tf, CHO-K1$^{GM3+}$ and CHO-K1$^{GD3+}$ cells were treated with P4, which is a potent inhibitor of UDP-Glc:ceramide glucosyltransferase (UGCG) and hence of the synthesis of glucosylceramide (GlcCer) and of more complex glycosphingolipids (refer to Fig. 1A). As shown in Figure 3B, general depletion of glycosphingolipids in CHO-K1$^{GM3+}$ cells did not affect the Tf endocytosis, as previously reported [36], whereas the same treatment in CHO-K1$^{GD3+}$ cells

led to a 30% reduction in Tf endocytosis. Overall, these results suggest that glycosphingolipids are not strictly necessary for CME of Tf, but they enhance the internalization of the cargo when they are more complex and have higher amounts of sialic acids. On the other hand, the drastic reduction of Tf endocytosis caused by NEU3 was still seen in glycosphingolipid-depleted cells, suggesting that NEU3 could operate in a way that is probably independent of its catabolic action on gangliosides.

### Tf uptake kinetics in NEU3 expressing cells

In the light of previous results, we decided to investigate further the participation of NEU3 in the endocytic process. The effect of NEU3 on Tf endocytosis was confirmed by a time lapse recording experiment in living cells. CHO-K1$^{GM3+}$ cells were transfected with the expression vector pTracerNEU3, which expresses NEU3 and GFP under independent promoters, thereby allowing transfected cells (GFP$^{+}$ cells) to be detected. Tf internalization in living CHO-K1$^{GM3+}$ cells transfected with pTracer vector (mock) was similar that in non-transfected cells (Fig. 4A, upper panels). In contrast, the ectopic expression of NEU3 induced a remarkable reduction in the kinetics of Tf uptake and its later accumulation in recycling endosomes (Fig. 4A, lower panels).

Tf uptake follows the general steps of receptor-mediated endocytosis. Diferric Tf binds to the Tf receptor (TfR) in the cell surface and concentrates in clathrin-coated pits. The Tf-TfR complex is internalized via CME in an endocytic vesicle, passing through early endosomes to recycling endosomes where iron dissociates from Tf. Most of the internalized iron free Tf-TfR complex is recycled back either from early endosomes, typically with a t1/2 of 2-3 min, or through a slower step via the recycling endosomes, with a $t_{1/2}$ of 10-15 min [37]. Previous reports have shown that a reduction in the total number of TfR leads to a decrease of Tf internalization [38, 39]. Since the first step of this process is the formation of the Tf-TfR complex, we analyzed the possibility that NEU3 could be reducing TfR levels at the cell surface. Thus, we measured the relative levels of Tf bound to its receptor at 4°C to ensure that the Tf-TfR complex remained at the plasma membrane without appreciable internalization [40]. CHO-K1$^{GM3+}$ cells expressing NEU3 were incubated with Tf-Alexa$^{647}$ for 30 min at 4°C, before being fixed and observed by confocal microscopy. As shown in Figure 4B, the Tf binding at the cell surface of NEU3 expressing cells was significantly reduced. More interestingly, experiments of Tf uptake performed at 16°C, widely used to accumulate the endocytic cargo in early endosomes, showed that NEU3 caused a notorious reduction of Tf content in this organelle (Fig. 4C). These results suggest that NEU3 interferes in an early step of the endocityc process.

### $\alpha_2$M, LDL and CTxβ endocytosis in NEU3 expressing cells

We next investigated if the internalization of other molecules could also have been affected by NEU3. Thus, we evaluated the uptake of fluorescent $\alpha_2$M, which binds to LRP1 (LDL receptor-Related Protein 1) and internalizes via CME [41, 42] and CTxβ, which binds to ganglioside GM1 before being internalized via both clathrin-independent and -dependent pathways [43-45]. Cells transiently expressing NEU3 were incubated with DMEM supplemented with $\alpha_2$M (60 nM) or CTxβ (0.2 µg/ml) for 30 min at 37°C, before being fixed and their ligand internalization analyzed by confocal microscopy. As shown in Figure 5A, NEU3 expressing cells had a remarkable reduction of $\alpha_2$M endocytosis, accounting for more than 50% of inhibition. It was also observed that NEU3 significantly affected the internalization of LDL, which after binding to its receptor is internalized through CME [46] (results not shown). In contrast, the expression of NEU3 did not significantly modify the internalization of CTxβ (Fig. 5B), which strongly suggests a close relationship between NEU3 activity and CME.

### NEU3 affects the distribution of clathrin adaptor AP-2 complex

After clathrin, the heterotetrameric clathrin adaptor complexes are the major protein components of clathrin-coated vesicles. Many studies have shown that adaptor protein 2 (AP-2; comprising α-, β2-, μ2-, and σ2- subunits) is the predominant clathrin adaptor at the plasma membrane, whereas similar protein complexes (AP-1, AP-3 and AP-4) have been shown to localize both in endosomes and Trans Golgi Network [3, 47]. AP-2 binds clathrin, cargo and PtdIns(4,5)$P_2$; it interacts directly with motifs in the cytoplasmic tails of transmembrane receptors through its μ2- and σ2-subunits, and also indirectly with cargoes using its globular C-terminal appendage domains to bind accessory adaptor proteins [1, 48-50]. Therefore, to explore in more details the mechanisms by which expression of NEU3 interferes with CME, we decided to examine its effect on AP-2 and clathrin subcellular distribution. To carry this out, clones with stable expression of EYFP-tagged clathrin light chain (CLC) and GFP-tagged σ2 subunit from AP-2 were generated in CHO-K1$^{GM3+}$ cells. These clones were transfected in order to ectopically express NEU3, before being fixed, immunostained to detect NEU3, and visualized by confocal microscopy. Images displayed the expected punctate pattern of AP-2 and CLC in NEU3 negative cells (Fig. 6A and 6B), which revealed clathrin-coated pits. As the expression of both fusion proteins had no effect on Tf uptake, this suggests that they did not interfere with the CME (results not shown). Interestingly, we observed that the AP-2 complex was mislocated and tended to accumulate in cells with ectopic expression of NEU3 (Fig. 6A) whereas no appreciable effect on clathrin localization was observed (Fig. 6B). The number of normal sized-AP-2 coated pits in NEU3 expressing cells resulted significantly reduced compared to the number of pits in non-transfected cells (Fig 6A). This can be attributed to the mislocalization and the major redistribution of AP-2 into larger clusters occurring in NEU3 expressing cells, while the number of clathrin coated pits were not modified by NEU3 (Fig. 6B).

On the other hand, and in line with results shown above, inhibition of the Tf endocytosis associated with NEU3 expression was also observed in cells from clones expressing AP-2 or CLC (results not shown). Additionally, the intracellular distribution of caveolin-1 in CHO-K1$^{GM3+}$ cells did not reveal any appreciable changes in cells expressing NEU3 (Fig. 6C). Taken together, these results suggest that the inhibitory effect of NEU3 on CME probably occurred by affecting the functional and structural organization of coated pits, associated with an abnormal subcellular distribution of AP-2.

### Effect of NEU3 expression on PtdIns(4,5)$P_2$ content

As mentioned above, AP-2 has binding sites for PtdIns(4,5)$P_2$ phosphoinositide[48]. In addition, other accessory proteins involved in CME also contain domains that mediate their binding to PtdIns(4,5)$P_2$-containing membranes (i.e. epsin, dynamin, AP180/CALM). The importance of this phosphoinositide for the assembly and stability of clathrin-coated pits at the cell surface was demonstrated by targeting an inositol 5-phosphatase to the plasma membrane, which caused the dissolution of clathrin-coated pits [51]. Furthermore, up-expression of NEU3 activates the phosphatidylinositide 3-kinase/Akt pathway in both renal cell carcinoma and HeLa cells [52, 53]. Taking all these findings into consideration, we explored whether NEU3 could have been exerting its effect on cargo internalization by regulating PtdIns(4,5)$P_2$ levels at the plasma membrane. Thus, CHO-K1$^{GM3+}$ cells were transfected to coexpress NEU3 and PH-PLCδ1-RFP, a PtdIns(4,5)$P_2$ probe. As shown in Figure 7, the expression of the sialidase did not modify the PtdIns(4,5)$P_2$ content or distribution at the cell surface, suggesting that the impairment of NEU3 in CME did not occur through the modulation of the cellular content of this phosphoinositide. As experimental controls, the expression of the PtdIns(4,5)$P_2$ probe did not modify Tf endocytosis (Fig. 7A) and, as expected, the probe dissociated from the plasma membrane after treatment of cells with ionomycin, a calcium ionophore that stimulates phosphoinositides hydrolysis (Fig. 7D).

## DISCUSSION

In the present study, we have shown the involvement of gangliosides and sialidase NEU3 in CME. In particular, we have provided evidence that gangliosides may have a role in CME, since the complexity and sialylation level of these glycolipids correlate with an enhancement of Tf internalization (Fig. 1C). Nevertheless, general depletion of glycosphingolipids in CHO-K1$^{GM3+}$ cells had no effect on Tf internalization, whereas reduced levels of glycolipid expression in cells that normally express the disialo-ganglioside GD3 (CHO-K1$^{GD3+}$) caused a reduction of 30% of Tf internalization. Thus, these results indicate that Tf internalization can occur even in absence of glycosphingolipids, but the presence of highly sialylated gangliosides increase the amount of internalized cargo via CME.

Other major point of this work is the fact that we have provided the first evidence of the involvement of sialidase NEU3 in CME. Indeed, we found that the ectopic expression of human NEU3 led to a drastic decrease in Tf endocytosis in all cell lines used in this study (Fig. 3), further suggesting a participation of gangliosides in this process. Nevertheless, the reduction of Tf endocytosis caused by NEU3 was even observed in glycosphingolipid-depleted cells, indicating that NEU3 modulated CME in a way that was probably independent of its action on gangliosides. Accordingly, we can consider that NEU3 may use sialoproteins as substrates, as has been previously suggested [23, 54], or eventually, might modify the biological properties of signal molecules by physical interaction, as already described for caveolin-1, Rac-1, Grb-2 and integrin β4 [55].

To assess whether the effect of NEU3 on CME is restricted to a specific cargo (Tf) or, in contrast, is a more general phenomenon, we evaluated the binding and internalization of $\alpha_2$M and LDL molecules (other markers for CME) in cells expressing NEU3. As observed for Tf, the ectopic expression of NEU3 dramatically reduced the uptake of these ligands, whereas NEU3 expression had no appreciable effect on CTxβ endocytosis (Fig. 5). Since CTxβ is endocytosed by both clathrin-dependent and -independent mechanisms, with caveolae being one of the major routes for its uptake [45, 56-58], this might explain why CTxβ endocytosis remains unaltered in NEU3 expressing cells. Furthermore, cells expressing NEU3 seem to have a typical intracellular distribution of caveolin-1 (Fig. 6C). Taken together, these results strongly suggest a specific and novel role of NEU3 in CME.

The effect of NEU3 on CME may be explained by a decrease in the total number of TfR at the cell surface, as previously demonstrated [38, 39]. In this sense, it was detected a significant reduction in Tf binding at 4°C (a well-established method for inhibiting endocytosis in mammalian cells) in NEU3 transfected cells, thus suggesting a reduction in the endogenous receptor at the plasma membrane (Fig. 4B). In addition, kinetic assays carried out in cells expressing the sialidase revealed a significant reduction in the sorting of endocytosed Tf to early and recycling endosomes (Fig. 4C). These findings prompted us to consider the possibility that NEU3 interferes in an early step of the endocytic process.

The formation of clathrin-coated vesicles is a complex process that involves a series of highly regulated steps. Cargo molecules, such as Tf and LDL, bind to membrane receptors having specific targeting sequences in their cytoplasmic tails, which are then involved in the recruitment to clathrin-coated pits through interaction with adaptor proteins [3, 48, 59]. Both clathrin and the AP-2 complex are major components of an endocytic clathrin coat with an imbalance in their functions being able to modify the normal endocytic process. In this context, previous reports have demonstrated that AP-2 is required for efficient Tf internalization by CME [60] and that AP-2 knockdown strongly inhibits receptor-mediated endocytosis of LDL and Tf [61]. Our results show that the expression of NEU3 resulted in a remarkable subcellular redistribution of AP-2, in comparison with the normal punctate and organized structures observed at the plasma membrane of neighboring cells that did not

express the sialidase (Fig. 6A). In contrast, clathrin recruitment into coated pits revealed no appreciable alteration in cells ectopically expressing NEU3 (Fig. 6B). It remains to be demonstrated whether NEU3 affect directly the association of AP-2 to coated pits or it results from an indirect consequence.

Phosphoinositide lipids play a central role in the organization and targeting of membrane traffic; in particular, PtdIns(4,5)$P_2$ is known to drive the plasma membrane localization of AP-2 [48]. Additionally, the overexpression of a mutant of epsin with a low affinity to PtdIns(4,5)$P_2$ , was previously shown to cause AP-2 to aggregate in the cytoplasm [62]. Based on these findings, we decided to explore the consequences of NEU3 expression on the PtdIns(4,5)$P_2$ content at the cell surface. The experiments revealed that the effect of NEU3 on CME probably did not occur by modifying the cellular content or the subcellular distribution of PtdIns(4,5)$P_2$ (Fig. 7).

Glycolipid expression results from a combination of biochemical processes and the occurrence of cross-talk among different enzymes involved in the metabolism of these lipids has been established [13, 54]. We demonstrated by real time qPCR that the ectopic expression of human NEU3 in CHO-K1$^{GM3+}$ cells resulted in changes in the levels of endogenous *NEU1*, *2* and *3* transcripts (Supplemental Fig. S2), with a similar tendency observed in the other CHO-K1 cell lines used in this work (data not shown). Consequently, this observation put into evidence the existence of a scenario even more complex, in which other members of the neuraminidase family should be also investigated to assess the specific role of NEU3 on CME.

In conclusion, this is the first demonstration showing a close relationship between a sialidase of gangliosides and CME. The displacement of the AP-2 complex produced by NEU3 expression, apparently independent of its catalytic activity on gangliosides, suggests a critical role of this adaptor protein in the reduction of cargo molecule endocytosis via clathrin-coated vesicles. Nevertheless, further studies are still needed to elucidate all the factors that induce redistribution of AP-2 and to determine the NEU3 role in this process.

## ACKNOWLEDGMENTS

The authors thank the technical assistance of C. Sampedro, C. Mas, G. Schachner and S. Deza. We also thank Dr. Paul Hobson, native speaker, for revision of the manuscript.

## AUTHOR CONTRIBUTION

M.R-W., A.A.V. and E.G-P. performed experiments. M.R-W, A.A.V. and J.L.D. conceived ideas, designed experiments, analysed results and wrote the manuscript. All authors edited and reviewed the final manuscript.

## FUNDING

This work was supported in part by Grants from Secretaría de Ciencia y Tecnología (SECyT), Universidad Nacional de Córdoba (UNC), Consejo Nacional de Investigaciones Científicas y Técnicas (CONICET) and Agencia Nacional de Promoción Científica y Tecnológica (ANPCyT), Argentina. M.R-W. is a recipient of CONICET (Argentina) fellowship. A.A.V., E.G-P. and J.L.D are career investigators of CONICET (Argentina).

## REFERENCES


1 McMahon, H. T. and Boucrot, E. (2011) Molecular mechanism and physiological functions of clathrin-mediated endocytosis. Nat. Rev. Mol. Cell Biol. **12**, 517-533

2 Sigismund, S., Confalonieri, S., Ciliberto, A., Polo, S., Scita, G. and Di Fiore, P. P. (2012) Endocytosis and signaling: cell logistics shape the eukaryotic cell plan. Physiol. Rev. **92**, 273-366

3 Edeling, M. A., Smith, C. and Owen, D. (2006) Life of a clathrin coat: insights from clathrin and AP structures. Nat. Rev. Mol. Cell Biol. **7**, 32-44

4 Donaldson, J. G., Porat-Shliom, N. and Cohen, L. A. (2009) Clathrin-independent endocytosis: a unique platform for cell signaling and PM remodeling. Cell Signal. **21**, 1-6

5 Hansen, C. G. and Nichols, B. J. (2009) Molecular mechanisms of clathrin-independent endocytosis. J. Cell Sci. **122**, 1713-1721

6 Howes, M. T., Mayor, S. and Parton, R. G. (2010) Molecules, mechanisms, and cellular roles of clathrin-independent endocytosis. Curr. Opin. Cell Biol. **22**, 519-527

7 Mayor, S. and Pagano, R. E. (2007) Pathways of clathrin-independent endocytosis. Nat. Rev. Mol. Cell Biol. **8**, 603-612

8 Daniotti, J. L. and Iglesias-Bartolome, R. (2011) Metabolic pathways and intracellular trafficking of gangliosides. IUBMB Life. **63**, 513-520

9 Daniotti, J. L., Vilcaes, A. A., Torres Demichelis, V., Ruggiero, F. M. and Rodriguez-Walker, M. (2013) Glycosylation of Glycolipids in Cancer: Basis for Development of Novel Therapeutic Approaches. Front. Oncol. **3**, 306

10 Yu, R. K., Tsai, Y. T., Ariga, T. and Yanagisawa, M. (2011) Structures, biosynthesis, and functions of gangliosides--an overview. J. Oleo Sci. **60**, 537-544

11 Maccioni, H. J. (2007) Glycosylation of glycolipids in the Golgi complex. J Neurochem. **103**, 81-90

12 Merrill, A. H., Jr. (2011) Sphingolipid and glycosphingolipid metabolic pathways in the era of sphingolipidomics. Chem. Rev. **111**, 6387-6422

13 Aureli, M., Masilamani, A. P., Illuzzi, G., Loberto, N., Scandroglio, F., Prinetti, A., Chigorno, V. and Sonnino, S. (2009) Activity of plasma membrane beta-galactosidase and beta-glucosidase. FEBS Lett. **583**, 2469-2473

14 Crespo, P. M., Demichelis, V. T. and Daniotti, J. L. (2010) Neobiosynthesis of glycosphingolipids by plasma membrane-associated glycosyltransferases. J. Biol. Chem. **285**, 29179-29190

15 Papini, N., Anastasia, L., Tringali, C., Croci, G., Bresciani, R., Yamaguchi, K., Miyagi, T., Preti, A., Prinetti, A., Prioni, S., Sonnino, S., Tettamanti, G., Venerando, B. and Monti, E. (2004) The plasma membrane-associated sialidase MmNEU3 modifies the ganglioside pattern of adjacent cells supporting its involvement in cell-to-cell interactions. J. Biol. Chem. **279**, 16989-16995

16 Vilcaes, A. A., Demichelis, V. T. and Daniotti, J. L. (2011) Trans-activity of plasma membrane-associated ganglioside sialyltransferase in mammalian cells. J. Biol. Chem. **286**, 31437-31446

17 Anastasia, L., Papini, N., Colazzo, F., Palazzolo, G., Tringali, C., Dileo, L., Piccoli, M., Conforti, E., Sitzia, C., Monti, E., Sampaolesi, M., Tettamanti, G. and Venerando, B. (2008) NEU3 sialidase strictly modulates GM3 levels in skeletal myoblasts C2C12 thus favoring their differentiation and protecting them from apoptosis. J. Biol. Chem. **283**, 36265-36271

18 Sonnino, S., Aureli, M., Loberto, N., Chigorno, V. and Prinetti, A. (2010) Fine tuning of cell functions through remodeling of glycosphingolipids by plasma membrane-associated glycohydrolases. FEBS Lett. **584**, 1914-1922

19 Kakugawa, Y., Wada, T., Yamaguchi, K., Yamanami, H., Ouchi, K., Sato, I. and Miyagi, T. (2002) Up-regulation of plasma membrane-associated ganglioside sialidase (Neu3) in human colon cancer and its involvement in apoptosis suppression. Proc. Natl. Acad. Sci. U S A. **99**, 10718-10723

20 Mandal, C., Tringali, C., Mondal, S., Anastasia, L., Chandra, S. and Venerando, B. (2010) Down regulation of membrane-bound Neu3 constitutes a new potential marker for childhood acute lymphoblastic leukemia and induces apoptosis suppression of neoplastic cells. Int. J. Cancer. **126**, 337-349

21 Rodriguez, J. A., Piddini, E., Hasegawa, T., Miyagi, T. and Dotti, C. G. (2001) Plasma membrane ganglioside sialidase regulates axonal growth and regeneration in hippocampal neurons in culture. J. Neurosci. **21**, 8387-8395

22 Miyagi, T. and Yamaguchi, K. (2012) Mammalian sialidases: physiological and pathological roles in cellular functions. Glycobiology. **22**, 880-896

23 Mozzi, A., Forcella, M., Riva, A., Difrancesco, C., Molinari, F., Martin, V., Papini, N., Bernasconi, B., Nonnis, S., Tedeschi, G., Mazzucchelli, L., Monti, E., Fusi, P. and Frattini, M. (2015) NEU3 activity enhances EGFR activation without affecting EGFR expression and acts on its sialylation levels. Glycobiology, doi:10.1093/glycob/cwv026

24 Wang, Y., Yamaguchi, K., Wada, T., Hata, K., Zhao, X., Fujimoto, T. and Miyagi, T. (2002) A close association of the ganglioside-specific sialidase Neu3 with caveolin in membrane microdomains. J. Biol. Chem. **277**, 26252-26259

25 Tringali, C., Lupo, B., Silvestri, I., Papini, N., Anastasia, L., Tettamanti, G. and Venerando, B. (2012) The plasma membrane sialidase NEU3 regulates the malignancy of renal carcinoma cells by controlling beta1 integrin internalization and recycling. J. Biol. Chem. **287**, 42835-42845

26 Giraudo, C. G., Rosales Fritz, V. M. and Maccioni, H. J. (1999) GA2/GM2/GD2 synthase localizes to the trans-golgi network of CHO-K1 cells. Biochem. J. **342 Pt 3**, 633-640

27 Iglesias-Bartolome, R., Crespo, P. M., Gomez, G. A. and Daniotti, J. L. (2006) The antibody to GD3 ganglioside, R24, is rapidly endocytosed and recycled to the plasma membrane via the endocytic recycling compartment. Inhibitory effect of brefeldin A and monensin. FEBS J. **273**, 1744-1758

28 Torres Demichelis, V., Vilcaes, A. A., Iglesias-Bartolome, R., Ruggiero, F. M. and Daniotti, J. L. (2013) Targeted delivery of immunotoxin by antibody to ganglioside GD3: a novel drug delivery route for tumor cells. PloS one. **8**, e55304

29 Wu, X., Zhao, X., Puertollano, R., Bonifacino, J. S., Eisenberg, E. and Greene, L. E. (2003) Adaptor and clathrin exchange at the plasma membrane and trans-Golgi network. Mol. Biol. Cell. **14**, 516-528

30 Crespo, P. M., Zurita, A. R. and Daniotti, J. L. (2002) Effect of gangliosides on the distribution of a glycosylphosphatidylinositol-anchored protein in plasma membrane from Chinese hamster ovary-K1 cells. J. Biol. Chem. **277**, 44731-44739

31 Wu, X., Zhao, X., Baylor, L., Kaushal, S., Eisenberg, E. and Greene, L. E. (2001) Clathrin exchange during clathrin-mediated endocytosis. J. Cell Biol. **155**, 291-300

32 Varnai, P. and Balla, T. (1998) Visualization of phosphoinositides that bind pleckstrin homology domains: calcium- and agonist-induced dynamic changes and relationship to myo-[3H]inositol-labeled phosphoinositide pools. J. Cell Biol. **143**, 501-510

33 Garbarino-Pico, E., Niu, S., Rollag, M. D., Strayer, C. A., Besharse, J. C. and Green, C. B. (2007) Immediate early response of the circadian polyA ribonuclease nocturnin to two extracellular stimuli. RNA. **13**, 745-755

34 Vandesompele, J., De Preter, K., Pattyn, F., Poppe, B., Van Roy, N., De Paepe, A. and Speleman, F. (2002) Accurate normalization of real-time quantitative RT-PCR data by geometric averaging of multiple internal control genes. Genome Biol. **3**, RESEARCH0034

35 Zhang, M., Koskie, K., Ross, J. S., Kayser, K. J. and Caple, M. V. (2010) Enhancing glycoprotein sialylation by targeted gene silencing in mammalian cells. Biotechnol. Bioeng. **105**, 1094-1105
36 Cheng, Z. J., Singh, R. D., Sharma, D. K., Holicky, E. L., Hanada, K., Marks, D. L. and Pagano, R. E. (2006) Distinct mechanisms of clathrin-independent endocytosis have unique sphingolipid requirements. Mol. Biol. Cell. **17**, 3197-3210
37 Maxfield, F. R. and McGraw, T. E. (2004) Endocytic recycling. Nat. Rev. Mol. Cell Biol. **5**, 121-132
38 Bourgeade, M. F., Silbermann, F., Thang, M. N. and Besancon, F. (1988) Reduction of transferrin receptor expression by interferon gamma in a human cell line sensitive to its antiproliferative effect. Biochem. Biophys. Res. Commun. **153**, 897-903
39 Leiter, L. M., Thatte, H. S., Okafor, C., Marks, P. W., Golan, D. E. and Bridges, K. R. (1999) Chloramphenicol-induced mitochondrial dysfunction is associated with decreased transferrin receptor expression and ferritin synthesis in K562 cells and is unrelated to IRE-IRP interactions. J. Cell Physiol. **180**, 334-344
40 Harding, C., Heuser, J. and Stahl, P. (1983) Receptor-mediated endocytosis of transferrin and recycling of the transferrin receptor in rat reticulocytes. J. Cell Biol. **97**, 329-339
41 Conner, S. D. and Schmid, S. L. (2003) Differential requirements for AP-2 in clathrin-mediated endocytosis. J. Cell Biol. **162**, 773-779
42 Wilsie, L. C., Gonzales, A. M. and Orlando, R. A. (2006) Syndecan-1 mediates internalization of apoE-VLDL through a low density lipoprotein receptor-related protein (LRP)-independent, non-clathrin-mediated pathway. Lipids Health Dis. **5**, 23
43 Chinnapen, D. J., Chinnapen, H., Saslowsky, D. and Lencer, W. I. (2007) Rafting with cholera toxin: endocytosis and trafficking from plasma membrane to ER. FEMS Microbiol. Lett. **266**, 129-137
44 Iglesias-Bartolome, R., Trenchi, A., Comin, R., Moyano, A. L., Nores, G. A. and Daniotti, J. L. (2009) Differential endocytic trafficking of neuropathy-associated antibodies to GM1 ganglioside and cholera toxin in epithelial and neural cells. Biochim. Biophys. Acta. **1788**, 2526-2540
45 Torgersen, M. L., Skretting, G., van Deurs, B. and Sandvig, K. (2001) Internalization of cholera toxin by different endocytic mechanisms. J. Cell Sci. **114**, 3737-3747
46 Marina-Garcia, N., Franchi, L., Kim, Y. G., Hu, Y., Smith, D. E., Boons, G. J. and Nunez, G. (2009) Clathrin- and dynamin-dependent endocytic pathway regulates muramyl dipeptide internalization and NOD2 activation. J. Immunol. **182**, 4321-4327
47 Peden, A. A., Oorschot, V., Hesser, B. A., Austin, C. D., Scheller, R. H. and Klumperman, J. (2004) Localization of the AP-3 adaptor complex defines a novel endosomal exit site for lysosomal membrane proteins. J. Cell Biol. **164**, 1065-1076
48 Canagarajah, B. J., Ren, X., Bonifacino, J. S. and Hurley, J. H. (2013) The clathrin adaptor complexes as a paradigm for membrane-associated allostery. Protein Sci. **22**, 517-529
49 Kelly, B. T., McCoy, A. J., Spate, K., Miller, S. E., Evans, P. R., Honing, S. and Owen, D. J. (2008) A structural explanation for the binding of endocytic dileucine motifs by the AP2 complex. Nature. **456**, 976-979
50 Ungewickell, E. J. and Hinrichsen, L. (2007) Endocytosis: clathrin-mediated membrane budding. Curr. Opin. Cell Biol. **19**, 417-425
51 Zoncu, R., Perera, R. M., Sebastian, R., Nakatsu, F., Chen, H., Balla, T., Ayala, G., Toomre, D. and De Camilli, P. V. (2007) Loss of endocytic clathrin-coated pits upon acute depletion of phosphatidylinositol 4,5-bisphosphate. Proc. Natl. Acad. Sci. U S A. **104**, 3793-3798
52 Bonardi, D., Papini, N., Pasini, M., Dileo, L., Orizio, F., Monti, E., Caimi, L., Venerando, B. and Bresciani, R. (2014) Sialidase NEU3 Dynamically Associates to

Different Membrane Domains Specifically Modifying Their Ganglioside Pattern and Triggering Akt Phosphorylation. PloS one. **9**, e99405

53 Ueno, S., Saito, S., Wada, T., Yamaguchi, K., Satoh, M., Arai, Y. and Miyagi, T. (2006) Plasma membrane-associated sialidase is up-regulated in renal cell carcinoma and promotes interleukin-6-induced apoptosis suppression and cell motility. J. Biol. Chem. **281**, 7756-7764

54 Valaperta, R., Chigorno, V., Basso, L., Prinetti, A., Bresciani, R., Preti, A., Miyagi, T. and Sonnino, S. (2006) Plasma membrane production of ceramide from ganglioside GM3 in human fibroblasts. FASEB J. **20**, 1227-1229

55 Miyagi, T., Wada, T. and Yamaguchi, K. (2008) Roles of plasma membrane-associated sialidase NEU3 in human cancers. Biochim. Biophys. Acta. **1780**, 532-537

56 Cho, J. A., Chinnapen, D. J., Aamar, E., te Welscher, Y. M., Lencer, W. I. and Massol, R. (2012) Insights on the trafficking and retro-translocation of glycosphingolipid-binding bacterial toxins. Front. Cell Infect. Microbiol. **2**, 51

57 Kenworthy, A. K., Petranova, N. and Edidin, M. (2000) High-resolution FRET microscopy of cholera toxin B-subunit and GPI-anchored proteins in cell plasma membranes. Mol. Biol. Cell. **11**, 1645-1655

58 Montesano, R., Roth, J., Robert, A. and Orci, L. (1982) Non-coated membrane invaginations are involved in binding and internalization of cholera and tetanus toxins. Nature. **296**, 651-653

59 Bonifacino, J. S. and Traub, L. M. (2003) Signals for sorting of transmembrane proteins to endosomes and lysosomes. Annu. Rev. Biochem. **72**, 395-447

60 Motley, A., Bright, N. A., Seaman, M. N. and Robinson, M. S. (2003) Clathrin-mediated endocytosis in AP-2-depleted cells. J. Cell Biol. **162**, 909-918

61 Boucrot, E., Saffarian, S., Zhang, R. and Kirchhausen, T. (2010) Roles of AP-2 in clathrin-mediated endocytosis. PloS one. **5**, e10597

62 Ford, M. G., Mills, I. G., Peter, B. J., Vallis, Y., Praefcke, G. J., Evans, P. R. and McMahon, H. T. (2002) Curvature of clathrin-coated pits driven by epsin. Nature. **419**, 361-366

## FIGURE LEGENDS

### FIGURE 1. Tf endocytosis in cell lines expressing different gangliosides

**A.** A schematic representation of ganglioside biosynthesis operating in wild-type CHO-K1 cells (CHO-K1$^{GM3+}$) and in CHO-K1 cell clones stably expressing ST8Sia-I (CHO-K1$^{GD3+}$) or β4GalNAcT-I and β3GalT-IV (CHO-K1$^{GD1a+}$). Glycosyltransferases that are stably expressed in each clone are underlined, the remaining are endogenously expressed by wild-type CHO-K1 cells. For a description of the enzymes and glycolipids depicted in this Figure, see [8, 12]. **B.** Cells were metabolically labeled with [$^{3}$H]galactose for 24 h. Lipid extracts were purified, chromatographed on an HPTLC plate and visualized as indicated in the Experimental section. The position of co-chromatographed radioactive ganglioside standards is indicated with brackets. Lipids migrate as multiple bands because of the heterogeneity of the fatty acyl chains in ceramide. Quantification of ganglioside content in each cell type is also shown. **C.** Cells grown on coverslips were incubated for 45 min at 37°C with Tf-Alexa$^{647}$ to allow the steady state distribution of internalized Tf. Then, cells were washed, fixed and visualized by confocal microscopy. To quantify Tf endocytosis, the whole fluorescence intensity of internalized Tf-Alexa$^{647}$ in cells (% respect to CHO-K1$^{GM3+}$) was analyzed using ImageJ software.

**FIGURE 2. Expression and characterization of human NEU3**

**A**. Western blot of total cell homogenate of CHO-K1$^{GM3+}$ and CHO-K1$^{GM3+,\ NEU3+}$ cells. Detection of NEU3 was carried out using anti-NEU3 or anti-c-Myc monoclonal antibodies. **B**. CHO-K1$^{GM3+}$ and CHO-K1$^{GM3+,\ NEU3+}$ cells were mechanically lysed, and the homogenates were ultra-centrifuged. NEU3 expression in both supernatant (S) and pellet (P) fractions was determined by Western blot using anti-NEU3 antibody. **C.** CHO-K1$^{GM3+,\ NEU3+}$ cells were immunostained with antibody to NEU3 (shown in green) and visualized by confocal microscopy. The average efficiency of cell transfection was 25-35%. Nuclei of cells were stained blue with Hoechst dye. **D**. Subcellular localization of NEU3 by immunofluorescence. Fixed and permeabilized CHO-K1$^{GM3+,\ NEU3+}$ cells transiently co-expressing NEU3 and LAMP1-GFP (a lysosome marker), Rab11-GFP (a recycling endosome marker), Rab5-GFP (an early endosome marker) or β4GalNAcT-I-Cherry (a Golgi marker) were immunostained with antibody to NEU3 and visualized by confocal microscopy. Organelle markers were analyzed by the intrinsic fluorescence of green and cherry fluorescent proteins. The inset is a merge of these images showing details at a higher magnification (NEU3 pseudo-colored in green and markers pseudo-colored in red). Manders' coefficient (green overlapped with red) is indicated at the bottom of each image. **E.** Analysis of NEU3 activity towards gangliosides (GD3, GD1a and GM1). Cells were incubated with antibody to GD3, antibody to GD1a or CTxβ (which binds to GM1) at 4°C for 60 min to label the plasma membrane-associated gangliosides. Then, cells were fixed, incubated with antibody to NEU3 and visualized by confocal microscopy. Ganglioside content was analyzed quantifying its fluorescence intensity using ImageJ software. Scale bars: 10 μm.

**FIGURE 3. Plasma membrane-bound sialidase NEU3 impairs the CME of Tf**

**A.** Cell lines expressing gangliosides with different levels of complexity and sialylation (CHO-K1$^{GM3+}$, CHO-K1$^{GD3+}$ and CHO-K1$^{GD1a+}$), transiently transfected with NEU3 and grown on coverslips were incubated for 45 min at 37°C with Tf-Alexa$^{647}$ to allow the steady-state distribution of internalized transferrin. Then, cells were washed and fixed. Both the uptake of Tf-Alexa$^{647}$ and the immunodetection of NEU3 were visualized by confocal microscopy. Insets show details at higher magnification of the internalized Tf in non-transfected and NEU3 transfected cells. **B.** Tf endocytosis in cells mentioned above was analyzed quantifying the whole fluorescence intensity of Tf-Alexa$^{647}$ (% respect to CHO-K1$^{GM3+}$) as indicated in Experimental section. As a reference, Tf uptake in non-transfected cells shown in Figure 1C is also included (diffuse white, gray and dark gray bars). Quantification of Tf-Alexa$^{647}$ uptake in CHO-K1$^{GM3+}$ and CHO-K1$^{GD3+}$ cells grown in a medium containing P4 (an inhibitor of glycosphingolipids biosynthesis) transiently transfected with NEU3. **C.** Tf endocytosis in CHO-K1 cells stably expressing NEU3 (CHO-K1$^{GM3+,\ GFP(NEU3)+}$) analyzed by Western blot as described in the Experimental section. GFP expression was used as a marker of cells stably expressing NEU3. Tubulin was used as a loading control. Densitometric quantification of internalized Tf-Alexa$^{647}$ and an immunofluorescence of NEU3 expressing cells (NEU3 in green and Hoechst dye labeling all nuclei in blue) are shown in the middle and right panels, respectively. The average yield of transfection of these stable cell lines correspond to about 55-60%. Scale bars: 10 μm.

**FIGURE 4. Tf uptake kinetics in NEU3 expressing cells**

**A**. Time lapse recording of Tf-Alexa$^{647}$ uptake at 37°C in living CHO-K1$^{GM3+}$ cells transiently transfected with pTracer vector (mock, CHO-K1$^{GM3+,\ GFP(Mock)+}$) or pTracerNEU3 (NEU3, CHO-K1$^{GM3+,\ GFP(NEU3)+}$). The boundaries of the cells (white dotted lines) are shown to facilitate discrimination between the Tf that is being endocytosed and the one that is outside the cells. Insets show details at higher magnification of the internalized Tf at 45 min in non-transfected and NEU3 transfected cells. Tf uptake kinetics was analyzed by quantifying the whole fluorescence intensity of Tf-Alexa$^{647}$ in cells (% respect to CHO-

$K1^{GM3+}$), using ImageJ software. **B**. CHO-$K1^{GM3+,\ GFP(NEU3)+}$ cells grown on coverslips were incubated for 30 min at 4°C with Tf-$Alexa^{647}$ to inhibit endocytic processes and to allow Tf binding at the cell surface. Then, cells were washed, fixed, and visualized by confocal microscopy. Insets show details at higher magnification of Tf binding in non-transfected and NEU3 transfected cells. Tf binding was measured by quantifying the fluorescence intensity of Tf-$Alexa^{647}$ using ImageJ software. **C.** CHO-$K1^{GM3+,\ NEU3+}$ cells grown on coverslips were incubated for 30 min at 20°C with Tf-$Alexa^{647}$ to allow Tf trafficking to early endosomes. Then, cells were washed, fixed, immunostained with antibody to NEU3 and visualized by confocal microscopy. The boundaries of the cells are shown with white dotted lines. Insets show details at higher magnification. Scale bars: 10 μm.

**FIGURE 5. Endocytosis of $\alpha_2$M and CTxβ**

**A.** CHO-$K1^{GM3+,\ NEU3+}$ grown on coverslips were incubated for 30 min at 37°C with $\alpha_2$M-$Alexa^{594}$. Then, cells were washed, fixed, immunostained with antibody to NEU3 and visualized by confocal microscopy. Insets show details at higher magnification of the internalized $\alpha_2$M in non-transfected and NEU3 transfected cells. $\alpha_2$M endocytosis was analyzed by quantifying the whole fluorescence intensity of $\alpha_2$M-$Alexa^{594}$ in cells (% respect to CHO-$K1^{GM3+}$) using ImageJ software. **B**. CHO-$K1^{GD1a+,\ NEU3+}$ cells grown on coverslips were incubated for 30 min at 37°C with CTxβ-$Alexa^{555}$. Then, cells were washed, fixed, immunostained with antibody to NEU3 and visualized by confocal microscopy. Insets show details at higher magnification of the internalized CTxβ in non-transfected and NEU3 transfected cells. CTxβ endocytosis was analyzed by quantifying the whole fluorescence intensity of CTxβ-$Alexa^{555}$ in cells (% respect to CHO-$K1^{GD1a+}$) using ImageJ software. Scale bars: 10 μm.

**FIGURE 6. Effect of NEU3 on AP-2, clathrin and caveolin-1 subcellular distribution**

**A.** CHO-$K1^{GM3+}$ cells stably expressing GFP-tagged σ2 subunit of AP-2 were transfected to transiently express NEU3, fixed, immunostained with antibody to NEU3 and analyzed by confocal microscopy. Insets show details at higher magnification of AP-2 distribution in non-transfected and NEU3 transfected cells. **B.** CHO-$K1^{GM3+}$ cells stably expressing EYFP-tagged clathrin light (CLC) chain were transfected to transiently express NEU3, fixed, immunostained with antibody to NEU3 and analyzed by confocal microscopy. **C.** CHO-$K1^{GM3+}$ cells were transfected to transiently express NEU3, fixed, immunostained with antibody to NEU3 and endogenous caveolin-1 and visualized by confocal microscopy. Quantification of the number of AP-2, CLC or caveolin-1 pits per cell area in CHO-$K1^{GM3+,\ NEU3+}$ cells (% respect to CHO-$K1^{GM3+}$ cells) is shown in **A**, **B** and **C**, respectively. Scale bars: 10 μm.

**FIGURE 7. Effect of NEU3 on the cellular content and membrane distribution of phosphoinositide PtdIns(4,5)$P_2$**

CHO-$K1^{GM3+}$ cells were co-transfected with pTracerNEU3 and PH-PLCδ1-RFP (a PtdIns(4,5)$P_2$ probe), incubated for 45 min at 37°C with Tf-$Alexa^{647}$ and visualized in vivo by confocal microscopy. **A.** Cells single transfected with the probe. **B.** Cells co-transfected with both plasmids. **C.** Membrane-bound PH-PLCδ1-RFP content in CHO-$K1^{GM3+,\ GFP(NEU3)+}$ with respect to CHO-$K1^{GM3+}$ cells was analyzed by quantifying the fluorescence intensity of the probe using ImageJ software. **D.** Hydrolysis of PtdIns(4,5)$P_2$ was stimulated by the addition of 10 μM ionomycin in the presence of 1.5 mM external calcium for 1 min at 37°C. PtdIns(4,5)$P_2$ hydrolysis is reflected in the redistribution of fluorescence from the membrane to the cytosol of PH-PLCδ1-RFP. Scale bars: 10 μm.

**FIGURE 1**

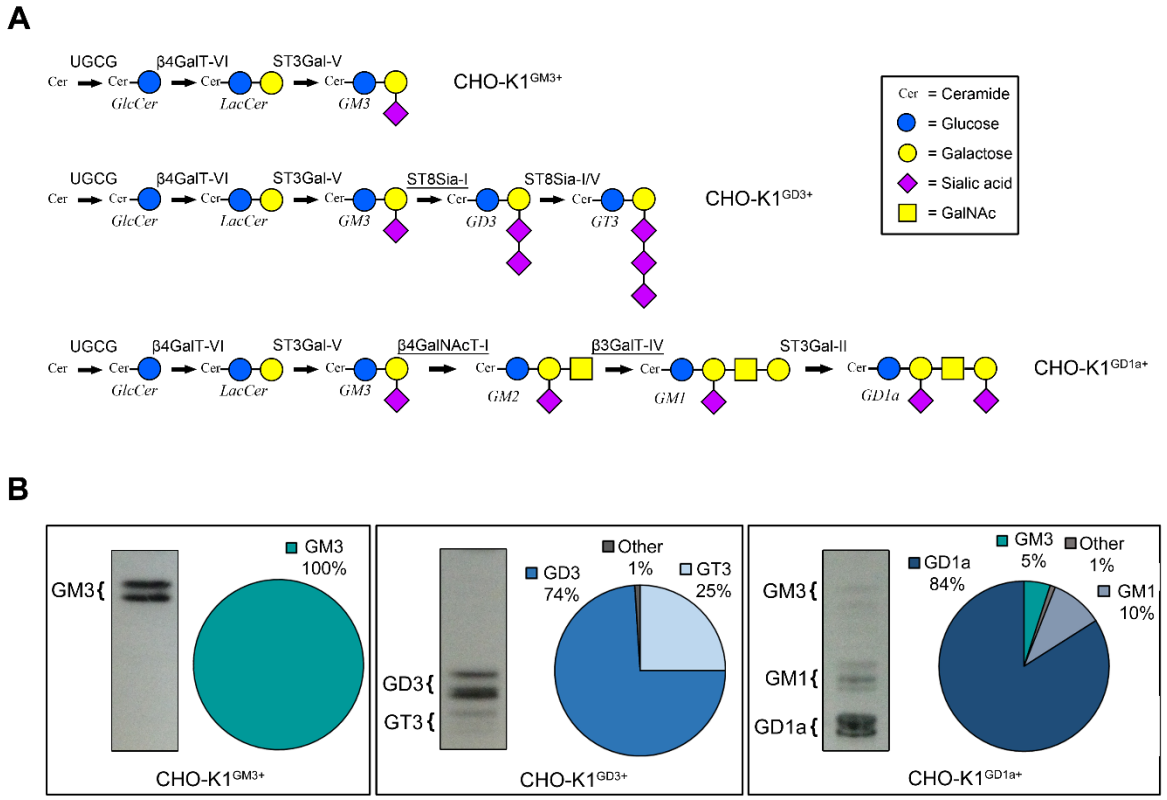
A
UGCG
β4GalT-VI
ST3Gal-V
Cer
GlcCer
LacCer
GM3
CHO-K1GM3+
ST8Sia-I
ST8Sia-I/V
GD3
GT3
CHO-K1GD3+
β4GalNAcT-I
β3GalT-IV
ST3Gal-II
GM2
GM1
GD1a
CHO-K1GD1a+
Cer = Ceramide
= Glucose
= Galactose
= Sialic acid
= GalNAc
B
GM3{
GM3
100%
CHO-K1GM3+
GD3{
GT3{
GD3
74%
Other
1%
GT3
25%
CHO-K1GD3+
GM1{
GD1a{
GD1a
84%
GM3
5%
Other
1%
GM1
10%
CHO-K1GD1a+
C
Tf endocytosis
200
180
160
140
120
100
80
60
40
20
0
*
*
CHO-K1GM3+
CHO-K1GD3+
CHO-K1GD1a+

**FIGURE 2**

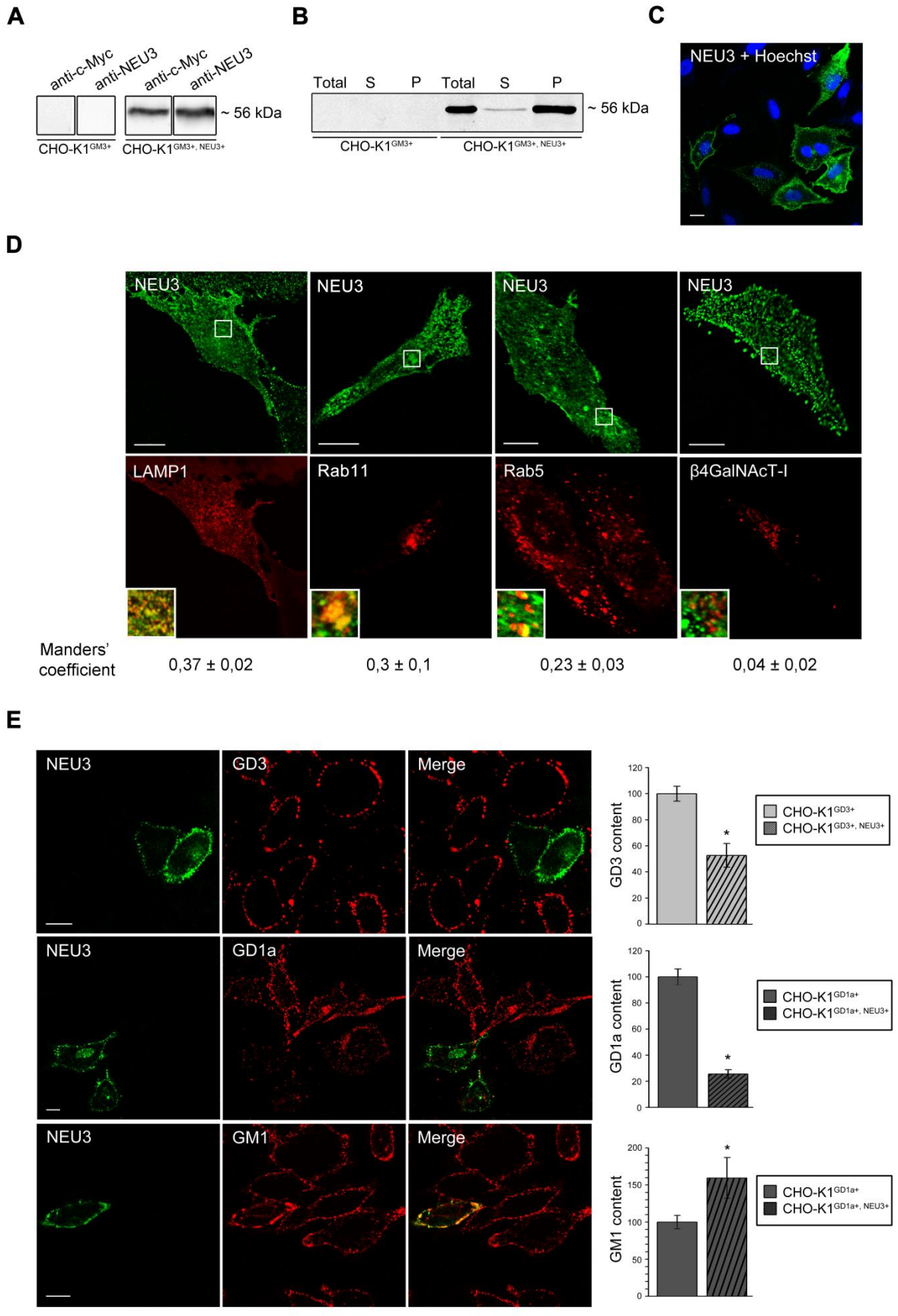
A
anti-c-Myc
anti-NEU3
anti-c-Myc
anti-NEU3
~ 56 kDa
CHO-K1GM3+
CHO-K1GM3+, NEU3+
B
Total S P Total S P
~ 56 kDa
CHO-K1GM3+
CHO-K1GM3+, NEU3+
C
NEU3 + Hoechst
D
NEU3
NEU3
NEU3
NEU3
LAMP1
Rab11
Rab5
β4GalNAcT-I
Manders' coefficient
0,37 ± 0,02
0,3 ± 0,1
0,23 ± 0,03
0,04 ± 0,02
E
NEU3
GD3
Merge
NEU3
GD1a
Merge
NEU3
GM1
Merge
GD3 content
CHO-K1GD3+
CHO-K1GD3+, NEU3+
GD1a content
CHO-K1GD1a+
CHO-K1GD1a+, NEU3+
GM1 content
CHO-K1GD1a+
CHO-K1GD1a+, NEU3+

**FIGURE 3**

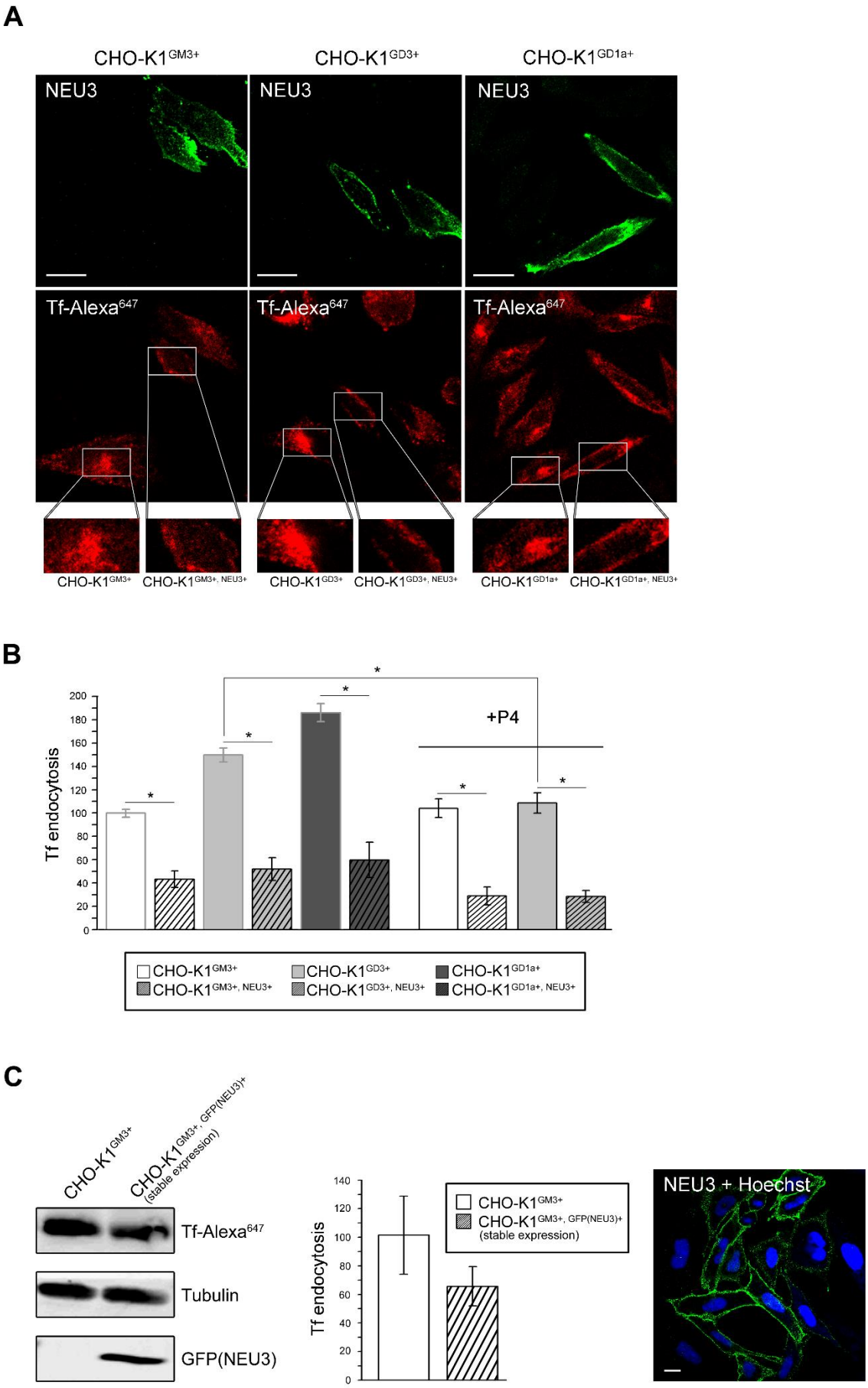
A
CHO-K1GM3+
CHO-K1GD3+
CHO-K1GD1a+
NEU3
Tf-Alexa647
CHO-K1GM3+
CHO-K1GM3+, NEU3+
CHO-K1GD3+
CHO-K1GD3+, NEU3+
CHO-K1GD1a+
CHO-K1GD1a+, NEU3+
B
Tf endocytosis
+P4
CHO-K1GM3+
CHO-K1GM3+, NEU3+
CHO-K1GD3+
CHO-K1GD3+, NEU3+
CHO-K1GD1a+
CHO-K1GD1a+, NEU3+
C
CHO-K1GM3+
CHO-K1GM3+, GFP(NEU3)+ (stable expression)
Tf-Alexa647
Tubulin
GFP(NEU3)
Tf endocytosis
NEU3 + Hoechst

**FIGURE 4**

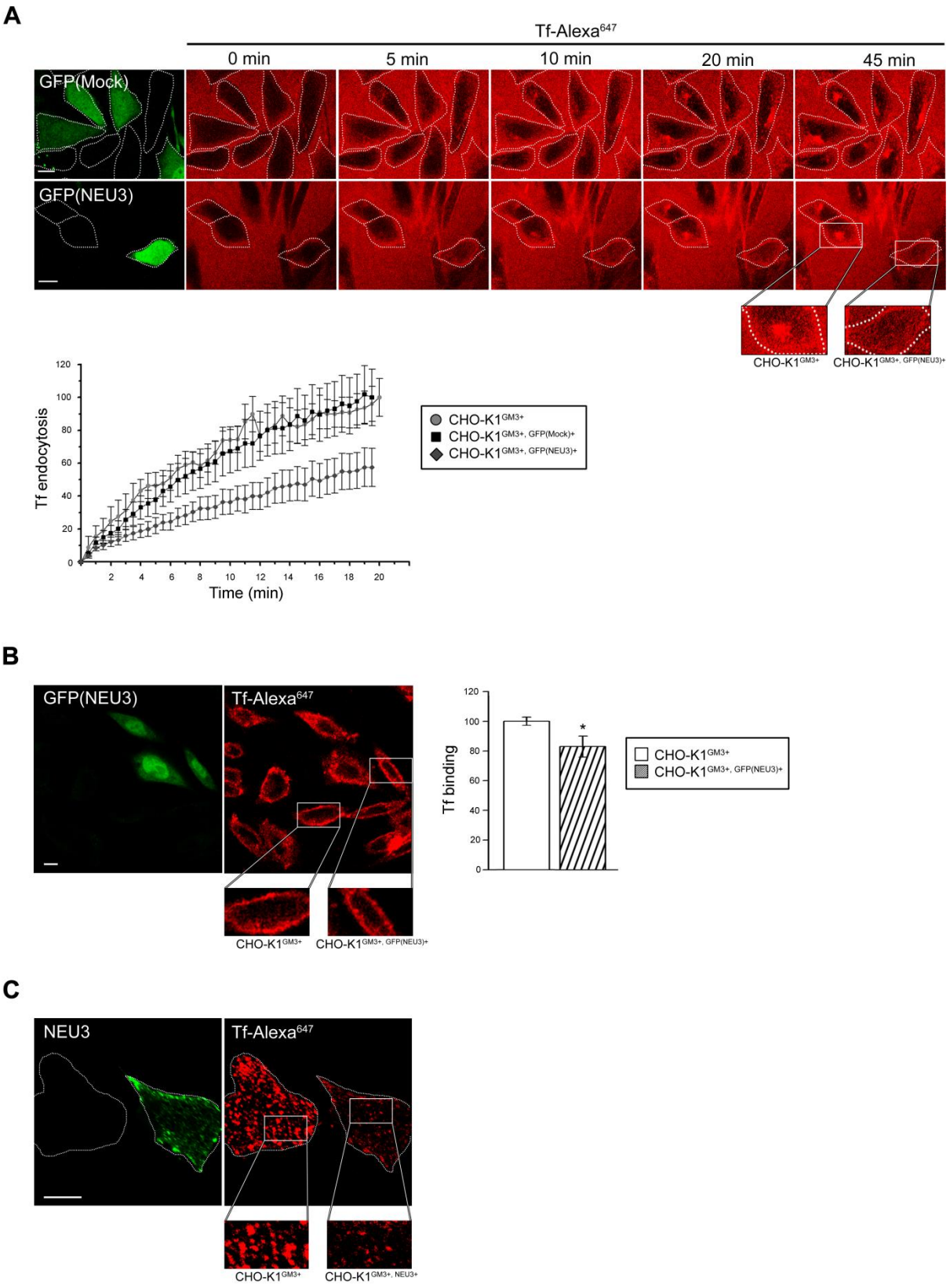
A
Tf-Alexa647
0 min
5 min
10 min
20 min
45 min
GFP(Mock)
GFP(NEU3)
CHO-K1GM3+
CHO-K1GM3+, GFP(NEU3)+
Tf endocytosis
Time (min)
CHO-K1GM3+
CHO-K1GM3+, GFP(Mock)+
CHO-K1GM3+, GFP(NEU3)+
B
GFP(NEU3)
Tf-Alexa647
CHO-K1GM3+
CHO-K1GM3+, GFP(NEU3)+
Tf binding
C
NEU3
Tf-Alexa647
CHO-K1GM3+
CHO-K1GM3+, NEU3+

**FIGURE 5**

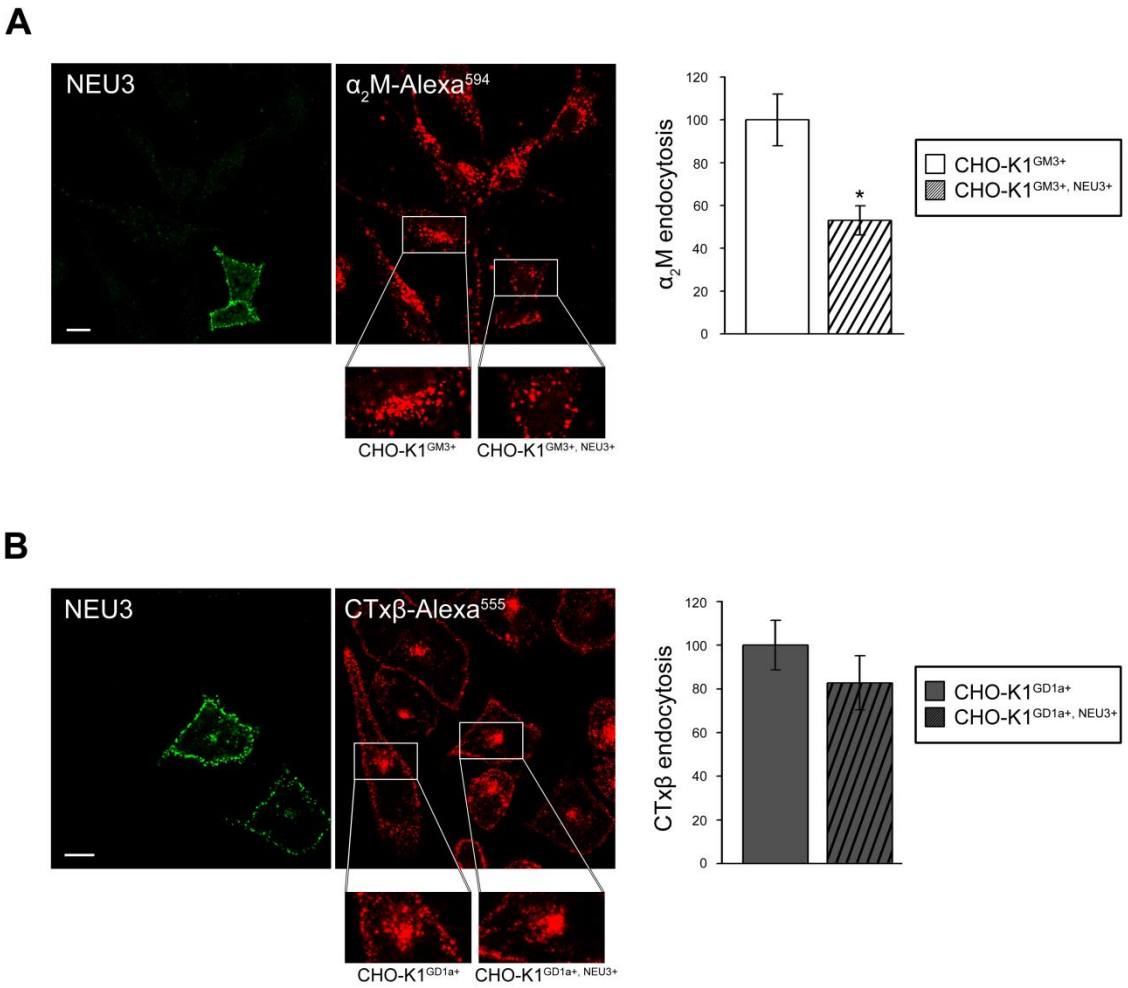
A
NEU3
α2M-Alexa594
CHO-K1GM3+
CHO-K1GM3+, NEU3+
α2M endocytosis
120
100
80
60
40
20
0
*
CHO-K1GM3+
CHO-K1GM3+, NEU3+
B
NEU3
CTxβ-Alexa555
CHO-K1GD1a+
CHO-K1GD1a+, NEU3+
CTxβ endocytosis
120
100
80
60
40
20
0
CHO-K1GD1a+
CHO-K1GD1a+, NEU3+

**FIGURE 6**

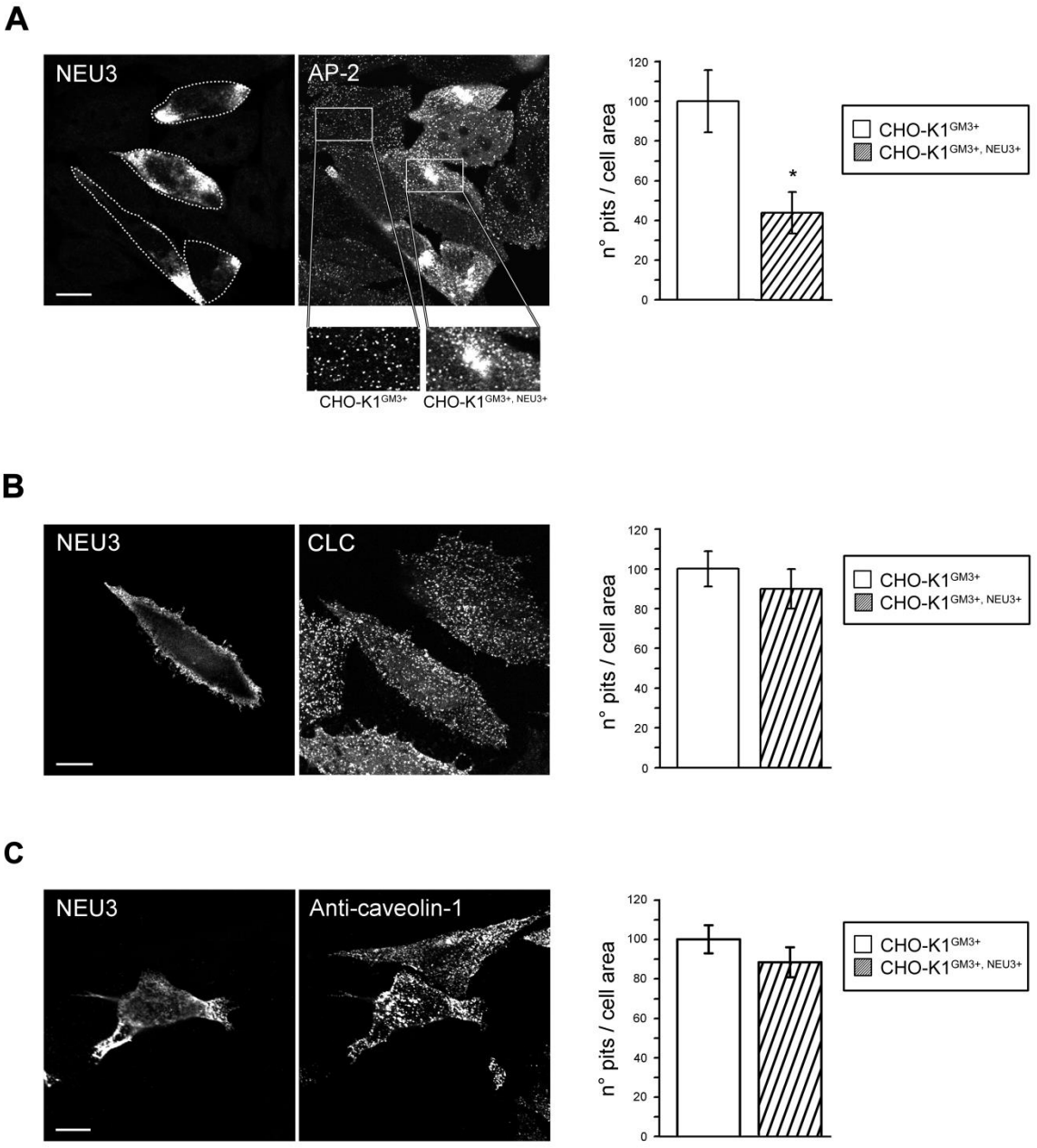
A
NEU3
AP-2
CHO-K1GM3+
CHO-K1GM3+, NEU3+
n° pits / cell area
120
100
80
60
40
20
0
*
CHO-K1GM3+
CHO-K1GM3+, NEU3+
B
NEU3
CLC
n° pits / cell area
CHO-K1GM3+
CHO-K1GM3+, NEU3+
C
NEU3
Anti-caveolin-1
n° pits / cell area
CHO-K1GM3+
CHO-K1GM3+, NEU3+

**FIGURE 7**

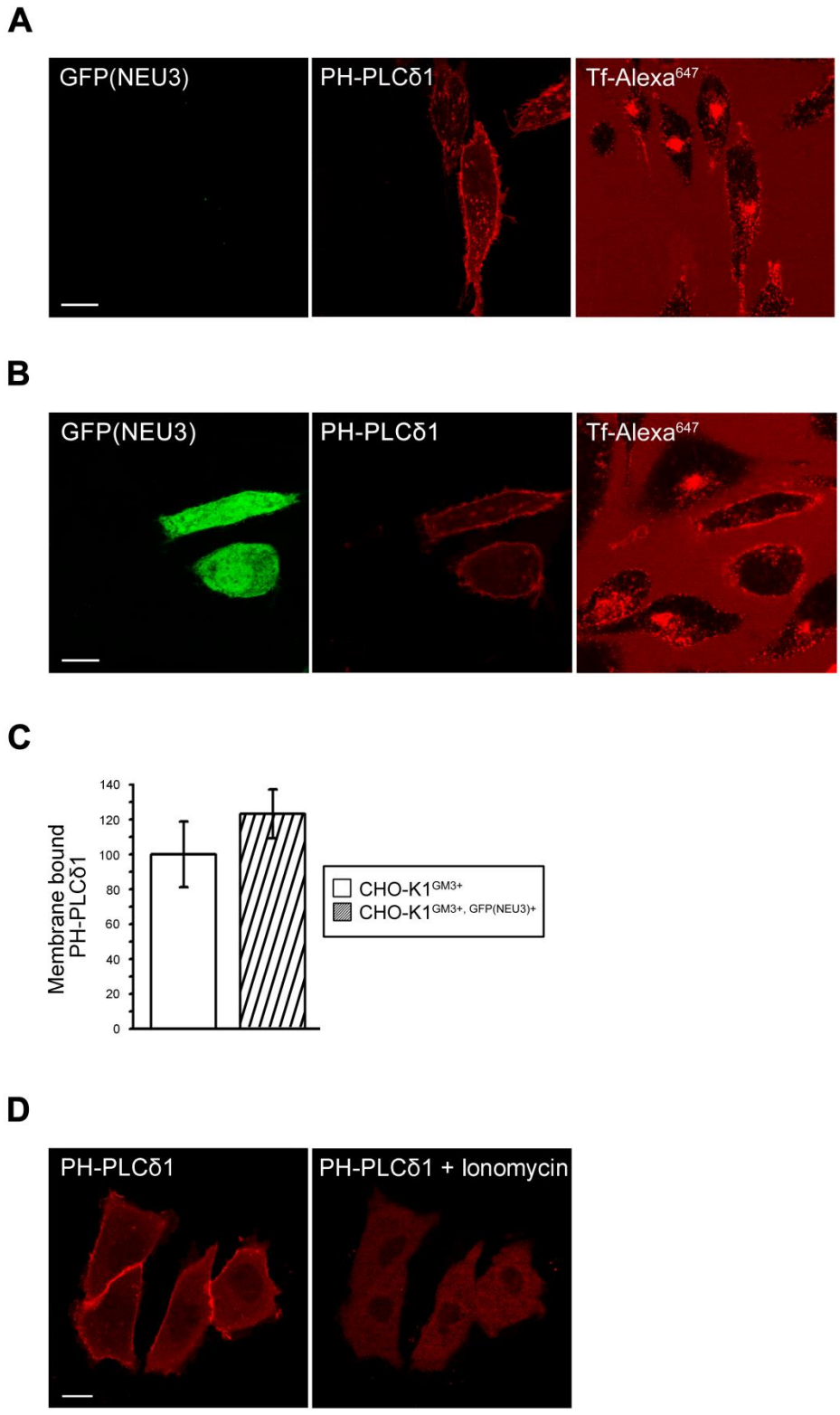
A
GFP(NEU3)
PH-PLCδ1
Tf-Alexa647
B
GFP(NEU3)
PH-PLCδ1
Tf-Alexa647
C
Membrane bound PH-PLCδ1
140
120
100
80
60
40
20
0
CHO-K1GM3+
CHO-K1GM3+, GFP(NEU3)+
D
PH-PLCδ1
PH-PLCδ1 + Ionomycin